

# High $Q$ light-emitting Si-rich $\text{Si}_3\text{N}_4$ microdisks

Federico Ferrarese Lupi,<sup>1,\*</sup> Daniel Navarro-Urrios,<sup>1</sup> Josep Monserrat,<sup>2</sup>  
Carlos Dominguez,<sup>2</sup> Paolo Pellegrino,<sup>1</sup> and Blas Garrido<sup>1</sup>

<sup>1</sup>MIND-IN2UB, Dept. Electrónica, Universitat de Barcelona, C/Marti i Franquès 1, 08028, Barcelona, Spain

<sup>2</sup>Instituto de Microelectrónica de Barcelona-Centre Nacional de Microelectrónica, Consejo Superior de Investigaciones Científicas, Bellaterra, E-08193, Barcelona, Spain

\*Corresponding author: fferrarese@el.ub.es

Received February 18, 2011; revised March 4, 2011; accepted March 4, 2011;  
posted March 8, 2011 (Doc. ID 142945); published April 6, 2011

We report on the optical properties of active silicon (Si)-rich  $\text{Si}_3\text{N}_4$  microdisk cavities in the visible range. We have studied the correlation between the quality ( $Q$ ) factor of the cavities and the active material deposition parameters. Microphotoluminescence measurements revealed subangstrom whispering gallery modes resonances and a maximum  $Q$  of  $10^4$  around 760 nm. These values improve significantly the best results reported so far for Si-based light-emitting circular resonators in the visible range. In contrast to what is reported for Si-rich  $\text{SiO}_2$ -based microcavities, we demonstrate the absence of a spectral widening at high pump fluxes associated to carrier absorption mechanisms, which allows high emitted power without degrading the  $Q$  of the cavity. These results open the route toward the monolithic integration of those structures into more complex circuits including Si photodetectors. © 2011 Optical Society of America

OCIS codes: 230.5750, 250.5230.

There is a broad agreement that silicon (Si) will become the future material for nanophotonics. The reason for this is that Si allows optical devices to be made cheaply using standard semiconductor fabrication techniques and integrated with microelectronic chips [1]. Among other applications, Si photonic structures and devices promise high bandwidth, densely integrated information systems with low operation and dissipation powers, as well as low-cost sensors with high sensitivity and specificity. However, one of the main drawbacks that explain why Si photonics is still not dominant with respect to compound semiconductors and Si microelectronics lies in the difficulties associated with making Si a host material for efficient light emission. Among the several alternatives to obtain highly efficient Si-based emitting materials, Si nanoclusters embedded in an  $\text{SiO}_2$  matrix has been probably the most investigated, since they can even provide optical gain in the visible region [2]. An interesting strategy has been to combine the light emission properties of those materials and the optical properties of circular microcavities (such as disks or rings) [3–6]. However, the work addressing this topic reveals maximum quality ( $Q$ ) factors on the emitted light of  $10^3$  [4–6] obtained at low pump powers, i.e., with low photoluminescence-emitted powers. Indeed, carrier absorption (CA) mechanisms decreased those  $Q$  at high pumping fluxes, thus limiting the possible applications of those devices [5,6]. Similarly to Si-rich  $\text{SiO}_2$ , Si-rich Si nitrides (SRSN) systems have also revealed efficient light emission in the visible range [7], in addition to a low barrier mismatch between Si and  $\text{Si}_3\text{N}_4$  that allows efficient electrical excitation [8]. Compact devices deposited over  $\text{SiO}_2$  cladding layers can be achieved with SRSN materials thanks to their relative high refractive indices ( $n \geq 2$ ). As an active medium for circular microcavities, SRSN has been only studied for applications in the IR region of the spectrum [9,10], aiming to exploit the sensitization effect when  $\text{Er}^{3+}$  ions are present in the matrix. In this Letter, we report an experimental characterization of visible light-emitting microdisks ( $\mu$ -disks) made of SRSN materials, in which  $Q$  values of about  $10^4$  have been measured with high emit-

ting powers, about three times greater than those made of Si-rich  $\text{SiO}_2$ .

The samples under analysis have been produced using standard complementary metal-oxide-semiconductor (CMOS) compatible processes. Initially,  $2\ \mu\text{m}$  of  $\text{SiO}_2$  was thermally grown ( $1100\ ^\circ\text{C}$ , wet ambient) on top of crystalline Si wafers, becoming the optical cladding of the active structures. A 300-nm-thick layer of stoichiometric  $\text{Si}_3\text{N}_4$  material was subsequently deposited by using the low-pressure chemical vapor deposition technique, which afterward suffered a Si ion implantation followed by an annealing in  $\text{N}_2$  atmosphere at  $1100\ ^\circ\text{C}$ . The thickness of the active material allows obtaining monomodal behaviors in the direction perpendicular to the disk surface for the transverse component of the electromagnetic field in the direction of the radius (TR) polarization (parallel to the disk surface). The implantation consisted of a 150 keV energy process (I1) followed by a second one at 90 keV with a lower dose (I2), aiming to obtain a flat Si excess profile. In Table 1, we summarize the active material parameters of the samples reported in this manuscript. Energy-filtered transmission electron microscopy measurements on sample 1 did not reveal Si crystalline nanostructures.

The photonic structures have been finally defined by means of standard photolithographic techniques. We have fabricated  $\mu$ -disks with radii ranging from 3 to  $10\ \mu\text{m}$  with average top surface roughness lower than 1 nm, as

**Table 1. Sample Parameters: Implantation Doses, Nominal Si Contents, and Associated Si Excess Values<sup>a</sup>**

Sample	I1/I2 Dose ( $\times 10^6\ \text{cm}^2$ )	Si Content (at. %)	Si Excess (%)
1	12.5/4.8	50	11.9
2	7.5/2.9	47.7	7.4
3	6.2/2.4	46.5	6.3
4	5.0/1.9	45.8	5.1

<sup>a</sup>The Si excess percentage is defined as  $(1 - 0.75x)/(1 + x)$ , where  $x$  is the ratio of the atomic concentrations of nitrogen and Si.

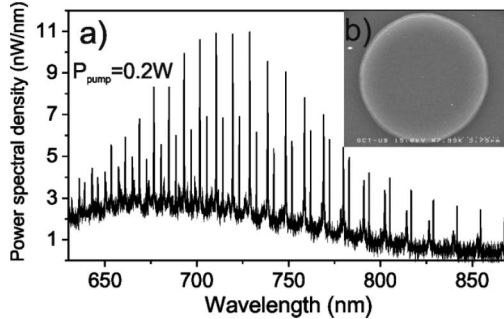


Fig. 1. (a) TR-polarized  $\mu$ -PL emission spectrum of a  $\mu$ -disk of sample 4 ( $R = 4.5 \mu\text{m}$ ). (b) SEM image of the corresponding  $\mu$ -disk.

extracted from atomic force microscopy (AFM) measurements. As an example, a scanning electron microscope (SEM) image of a  $\mu$ -disk with a radius ( $R$ ) of  $4.5 \mu\text{m}$  is shown in Fig. 1(b). Waveguides with different widths ( $1\text{--}10 \mu\text{m}$ ) have been also produced in order to characterize the optical losses of the active material. Those measurements have been done by using the cutback technique at  $633$  and  $780 \text{ nm}$ .

High spectral resolution microphotoluminescence ( $\mu$ -PL) experiments were performed at room temperature with the goal of characterizing the on-plane spectral emission of a single  $\mu$ -disk. We have used the  $476 \text{ nm}$  line of an Argon laser and a solid state laser emitting at  $370 \text{ nm}$  as excitation sources. A long working distance objective was used to focus the laser beam on the top surface of the disks providing a spot size of few micrometers. Another objective ( $\text{NA} = 0.4$ ) was used to collect the on-plane  $\mu$ -PL emission, which was afterward focused on a high-resolution monochromator ( $\Delta\lambda = 0.06 \text{ nm}$ ) coupled to a visible CCD camera. A linear polarizer was also placed in the collection line to select the TR or TM polarized emission. Finally, the total on-plane emission has been quantified by measuring the signal collected by the objective (which only collects a finite solid angle) with a calibrated photodetector, and then integrating to the  $2\pi$  angle in which the on-plane  $\mu$ -disk emission is distributed. It is worth mentioning that we are currently optimizing a structure in which an  $\text{Si}_3\text{N}_4$  waveguide is placed below the  $\mu$ -disks, aiming to extract the emitted power efficiently without damaging the quality of the cavities.

The main panel of Fig. 1 reports the quantified  $\mu$ -PL spectrum (TR polarized) obtained under a  $476 \text{ nm}$  pumping from a single  $\mu$ -disk with  $R = 4.5 \mu\text{m}$ , being the active material of sample 4. Whispering gallery mode resonances are clearly observable over an offset PL signal that has the same spectral shape of the PL emission obtained from the bulk material. The latter signal is not coupled to supported modes of the disk. The area of the curve provides a total power emitted on plane of  $0.6 \mu\text{W}$  ( $0.12 \mu\text{W}$  contained within the resonances), associated with a minimum power efficiency of  $\sim 3 \times 10^{-6}$ . We have measured an order of magnitude higher efficiency ( $\sim 3 \times 10^{-5}$ ) by decreasing the pumping wavelength to  $370 \text{ nm}$ , which is a result of the increasing of the excitation cross section of the emitting species. Those efficiency values can be much further improved by optimizing the overlap of the pumping spot shape and the emitting region within the disk that is

actually coupled to the supported modes. In fact, the calculated modal volumes for the fundamental modes (few cubed micrometers) are much smaller than the pumped volume (several tens of cubed micrometers).

We have studied the performance of the active materials associated with the different samples in terms of three magnitudes: (i) PL of the bulk material, (ii) optical losses of the waveguides, and (iii)  $Q$  of the  $\mu$ -disk. The latter is inversely proportional to the internal losses ( $\alpha$ ) within the resonator ( $Q = \lambda/\Delta\lambda = 2\pi n_g/\lambda\alpha$ , where  $n_g$  is the group refractive index of the mode).

Regarding the PL spectra (not reported here), we have observed that the PL intensity roughly scales with the pumping flux and the implantation dose. On the other hand, we have determined that the propagation losses on the waveguides increase: (i) with the Si excess (red circles in Fig. 2(a)) and (ii) roughly by a factor of 2 when moving to  $633 \text{ nm}$ . The first behavior seems directly related with the inverse of the  $Q$  values of the  $\mu$ -disks, as also shown in Fig. 2(a). In Fig. 2(b), we illustrate this effect for the cases of sample 1 and sample 4 ( $R = 7.5 \mu\text{m}$  in both cases). Resonances on sample 1 appear much wider than those of sample 4, in which a multimodal behavior observed is associated with several radial modes of different order. In fact, the maximum  $Q$  values are those corresponding to sample 4, which has lower Si excess. In this case, subangstrom resonances are observed on a spectral range of several tens of nanometers around  $760 \text{ nm}$ , leading to  $Q$  values as high as  $10^4$  (see Fig. 2(c)). Those  $Q$  values are, to the best of our knowledge, the best ones reported so far in light-emitting Si-based circular microresonators in the visible range. We address the material losses as the limiting factor for the measured  $Q$  values since there is a strong dependence on the Si excess present in the matrix and a clear correlation with the inverse of the optical losses of the waveguides [11]. Furthermore, we observed a decreasing of  $Q$  at lower

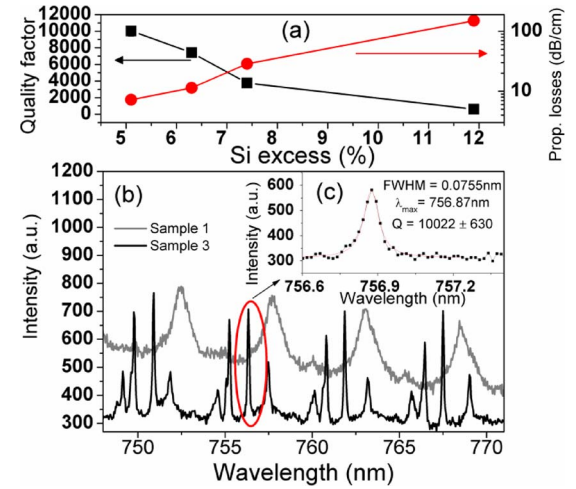


Fig. 2. (Color online) (a) Behavior of  $Q$  (black squares) around  $760 \text{ nm}$  as function of the Si excess for  $R = 7.5 \mu\text{m}$ . Propagation losses at  $780 \text{ nm}$  are also reported (red circles). (b) TR-polarized  $\mu$ -PL spectrum corresponding to disks with  $R = 7.5 \mu\text{m}$  of samples 1 (gray) and 4 (black). (c) Resonance present at  $756.87 \text{ nm}$  for sample 4 together with the corresponding Lorentzian fit.

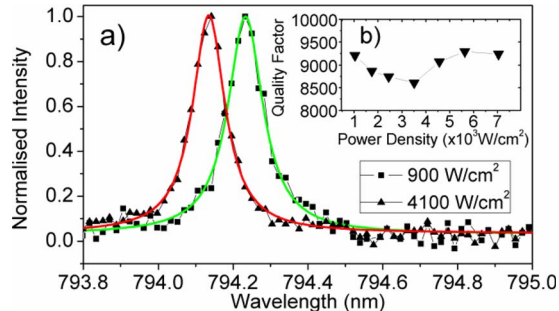


Fig. 3. (Color online) (a)  $\mu$ -PL spectra of a resonance at 794 nm for a  $10\ \mu\text{m}$  disk in sample 4 at low (squared points) and high (triangular points) power densities. (b)  $Q$  as a function of the pump power density.

wavelengths, in agreement with the mentioned increasing of the optical losses.

We have also investigated the effect that the pumping power may induce the optical losses of the material and, therefore, the  $Q$  values of the cavities. Indeed, in the case of Si-rich  $\text{SiO}_2$   $\mu$ -disk systems, CA losses prevail at high pumping fluxes, which is mainly a consequence of the relatively long lifetime (tens of microseconds) of the excited carriers (in situations where Auger or stimulated emission processes are not dominant mechanisms) [12]. On the contrary, in SRSN  $\mu$ -disks, CA mechanisms do not dominate the total losses of the material. In Fig. 3, we show the results of a  $\mu$ -disk of sample 4 ( $R = 10\ \mu\text{m}$ ): the  $Q$  values remain around 9000 over a wide range of pumping powers. We have also experimentally established an upper limit to the decay lifetime of the PL emission of 200 ns (the temporal resolution of our experimental set-up), almost 2 orders of magnitude faster than in Si-rich  $\text{SiO}_2$ . It is worth noting that the authors in [13] report a maximum recombination lifetime of 50 ns. Therefore, the total recombination probability of the carriers generated in this material is so high that CA effects do not generate measurable losses, so that  $Q$  values do not decrease. An immediate implication is that it is possible to have high emitted power with high  $Q$ , in contrast to what occurs in Si-rich  $\text{SiO}_2$ . In fact, we have measured that the power contained by a single resonance in the range between 700 and 770 nm can be as high as a few nanowatts (e.g., see Fig. 1), while keeping  $Q$  factors close to  $10^4$ . On the other hand, free carrier refraction effects at high powers are not totally absent since they are likely originating a slight decreasing of the material refractive index that produces the subnanometer blueshift reported in Fig. 3.

In conclusion, we have done a thorough study of Si-rich  $\text{Si}_3\text{N}_4$   $\mu$ -disk resonators, where we have quantified on-plane emitted powers up to  $0.6\ \mu\text{W}$  (few nanowatts in a single resonance) and measured  $Q$  values of  $10^4$  on a wide spectral range around 760 nm. We have also established a direct relationship among the Si excess, the waveguide optical losses, and the inverse of the  $Q$  of

the cavities. In addition, we have demonstrated that an increasing of the pumping flux does not generate a spectral widening of the resonances, which is in contrast to that observed in other reports of Si-rich  $\text{SiO}_2$ -based  $\mu$  cavities. The present result allows high emitted power within the resonances while maintaining  $Q$  values close to  $10^4$ . Indeed, these power values are well above the minimum sensibility of state-of-the-art visible Si-based integrated photodetectors [14], which would allow detecting the emitted signal within the same chip. On the basis of these results, we foresee the use of visible light-emitting SRSN  $\mu$ -disk resonators as CMOS-compatible integrated light sources in photonic platforms with increased complexity for sensing and telecommunications applications.

We acknowledge the Spanish Ministry of Science and Innovation projects GICSERV NGG-172 and TEC 2008-08359 for financial support. D. Navarro-Urrios thanks the Spanish Ministry of Science and Innovation through the Juan de la Cierva program.

## References and Notes

1. Nat. Photon. **4**, 491 (2010).
2. L. Pavesi, S. Gaponenko, and L. Dal Negro, eds. *Towards the First Silicon Laser*, NATO Science Series (Kluwer, 2003), Vol. 93.
3. R.-J. Zhang, S.-Y. Seo, A. P. Milenin, M. Zacharias, and U. Gösele, Appl. Phys. Lett. **88**, 153120 (2006).
4. P. Biancucci, X. Wang, J. G. C. Veinot, and A. Meldrum, Opt. Express **18**, 8466 (2010).
5. M. Ghulinyan, D. Navarro-Urrios, A. Pitanti, A. Lui, G. Pucker, and L. Pavesi, Opt. Express **16**, 13218 (2008).
6. R. D. Kekatpure and M. Brongersma, Nano Lett. **8**, 3787 (2008).
7. L. D. Negro, J. H. Yi, J. Michel, L. C. Kimerling, T. F. Chang, V. Sukhovatkin, and E. H. Sargent, Appl. Phys. Lett. **88**, 233109 (2006).
8. J. Warga, R. Li, S. Basu, and L. D. Negro, Appl. Phys. Lett. **93**, 151116 (2008).
9. J. S. Chang, S. C. Eom, G. Y. Sung, and J. H. Shin, Opt. Express **17**, 22918 (2009).
10. J. H. Shin, M.-S. Yang, J.-S. Chang, S.-Y. Lee, K. Suh, H. G. Yoo, Y. Fu, and P. Fauchet, Proc. SPIE **6897**, 68970N (2008).
11.  $Q_{\text{rad}}$ ,  $Q_{\text{ssc}}$ , and  $Q_{\text{sa}}$  contributions to the total  $Q$  (related to the radiation absorption and volume scattering losses, respectively) should be independent of the Si excess for the same  $\mu$ -disk radius. The low top surface roughness measured by AFM measurements and the high  $Q_{\text{rad}}$  extracted from finite-difference time-domain simulations ( $Q_{\text{rad}} > 10^6$  for  $R > 5\ \mu\text{m}$ ) allows us to disregard their contribution.
12. D. Navarro-Urrios, A. Pitanti, N. Daldosso, F. Gourbilleau, R. Rizk, G. Pucker, and L. Pavesi, Appl. Phys. Lett. **92**, 051101 (2008).
13. R. Li, J. Schneck, J. Warga, L. Ziegler, and L. D. Negro, Appl. Phys. Lett. **93**, 091119 (2008).
14. S. Assefa, F. Xia, W. M. J. Green, C. L. Schow, A. V. Rylyakov, and Y. A. Vlasov, IEEE J. Sel. Top. Quantum Electron. **16**, 1376 (2010).